

Graph Inference Towards ICD Coding

1st Xiaoxiao Deng

College of Computing and Digital Media

DePaul University

Chicago, United States

dengxiaoxiao1019@gmail.com

Abstract—Automated ICD coding involves assigning standardized diagnostic codes to clinical narratives. The vast label space and extreme class imbalance continue to challenge precise prediction. To address these issues, LabGraph is introduced—a unified framework that reformulates ICD coding as a graph generation task. By combining adversarial domain adaptation, graph-based reinforcement learning, and perturbation regularization, LabGraph effectively enhances model robustness and generalization. In addition, a label graph discriminator dynamically evaluates each generated code, providing adaptive reward feedback during training. Experiments on benchmark datasets demonstrate that LabGraph consistently outperforms previous approaches on micro-F1, micro-AUC, and P@K.

Index Terms—transfer learning, graph convolutional network, lightweight attention, ICD code prediction, adversarial domain adaptation

I. INTRODUCTION

Automated ICD coding has gained attention for its potential to reduce manual effort in clinical documentation and billing. Patient records contain diverse information, including admissions, physician notes, medical history, and lab tests [1]. As illustrated in Figure 1, ICD codes are organized hierarchically, with sibling codes rarely co-occurring in a single record. This sparse, hierarchical structure poses challenges for models, which must capture both semantic relationships and code dependencies for accurate prediction.

Automated ICD coding is typically handled as a multi-label prediction task using neural network techniques [2]. Automated ICD coding faces several key challenges. First, the label distribution is extremely imbalanced: out of 9,219 possible codes, only 122 appear frequently within the top 50 categories, leaving the majority of codes sparsely represented in clinical records. Second, crucial connections between codes—like sibling associations, mutually exclusive pairs, and hierarchical parent-child links—are frequently overlooked or

inadequately modeled [3]. For instance, “783.1” (Abnormal weight gain) and “783.2” (Abnormal weight loss) cannot logically co-occur, yet such constraints are rarely considered in existing systems. Third, relying on a single training strategy can limit model performance, particularly for rare disorders that appear infrequently in the data [4].

To address challenges in automated ICD coding, we reformulate the task as labeled graph generation over the ICD code hierarchy. A global code graph is first constructed from training labels, and initial labels are generated from the root node based on clinical text input. Subsequent labels are predicted using neighboring nodes and embeddings, reducing the candidate space. We propose LabGraph, a multi-component framework with four training strategies, comprising six modules: Label Graph Generator (LGG), Label Graph Discriminator (LGD), Message Integration Module (MIM), MHR-CNN, Fat-RGCN, and an adversarial adaptive training mechanism. MIM captures semantic and structural relationships, LGG generates labels resembling ground truth, and LGD discriminates between generated and authentic labels for training.

We also enhance knowledge graph representation learning to map entities and relations into dense, low-dimensional vector spaces. Building on existing resources such as DBpedia [5], YAGC [6], and Freebase [7], we extend representation learning to both one-hop and multi-hop neighbor subgraphs. In one-hop aggregation, both neighbor nodes and edges, as well as their influence on central node representations, are considered. Multi-hop subgraphs allow adaptive embedding of central nodes beyond the limitations of single-hop neighborhoods. These two levels of aggregation are fused into the Fat-RGCN module.

We isolate and evaluate each module’s contribution inside the enhanced knowledge representation framework using a series of ablation tests to confirm the efficacy of our suggested methodology. To determine the value of integrating the two algorithmic improvements, we also analyze their combined performance. To give thorough empirical proof of LabGraph’s performance, extensive tests are conducted on the MIMIC-III benchmark dataset [8]. According to Table I, LabGraph outperforms current state-of-the-art techniques in every important evaluation criteria.

Main contributions of this study are summarized as follows:

- Automatic EHR coding is reframed as a labeled graph generation problem, with LabGraph introduced as a unified multi-algorithm framework for ICD code prediction.

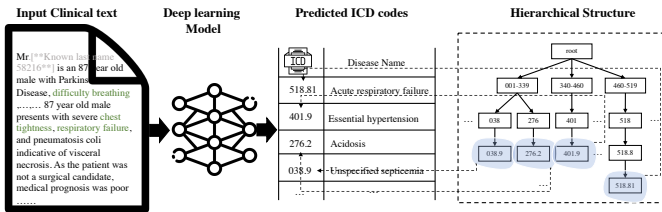


Fig. 1. ICD-9 code hierarchy and example of automatic ICD coding, with clinical text as input and predicted codes as output.

condenses memory representations while retaining hierarchical information, effectively capturing both local semantic features and global code dependencies for improved prediction accuracy.

BI-GRU [18] & HA-GRU [19]: BI-GRU generates informative EHR embeddings for binary ICD classification; HA-GRU extends BI-GRU with hierarchical attention to improve disease categorization.

CAML & DR-CAML [20]: CAML uses convolutional attention networks to learn ICD embeddings; DR-CAML adds label-wise normalization with regularization to enhance performance.

LAAT & JointLAAT [4]: LAAT applies label-specific attention on LSTM hidden states for ICD classification; JointLAAT adds hierarchical joint learning to improve efficiency and accuracy.

ISD [21], MSMN [22], & FUSION [23]: ISD uses interactive shared representations to tackle long-tail issues; MSMN applies synonym matching and data augmentation to enhance embedding learning; FUSION addresses sparse diagnosis vocabularies via attention-based modeling of local and global features.

D. Graph Generation Mechanism

The ICD code generation process follows a hierarchical path from root to leaf nodes. Given input text X , at each step t :

1. State Encoding: Current state s_t encodes the partial path (c_1, \dots, c_{t-1}) and text features
2. Action Space Reduction: Valid actions \mathcal{A}_t are restricted to children of c_{t-1} in the ICD hierarchy
3. Policy Network: $\pi(a_t|s_t, X)$ selects next code based on text-code alignment scores
4. Termination: Generation stops when a leaf node is reached or a cycle forms

This formulation reduces the search space from $O(\text{---C---})$ to $O(k)$, where k is the average branching factor, addressing the computational challenges of large label spaces.

E. Computational Analysis

Time complexity: $\mathcal{O}(L \cdot k \cdot d)$ where L is path length, k is branching factor, d is embedding dimension. This compares favorably to flat classification $\mathcal{O}(|C| \cdot d)$ when $k \ll |C|$.

Space complexity: $\mathcal{O}(|V| + |E|)$ for storing the ICD graph, plus $\mathcal{O}(B \cdot L \cdot d)$ for batch processing, where B is batch size.

Inference time on MIMIC-III: 0.23s per document (vs. 0.18s for CAML), showing practical efficiency despite increased model complexity.

IV. RESULT AND ANALYSIS

ICD code distribution varies across levels: fourth-level codes account for 40.1% of MIMIC-III Top50, while first- to third-level codes make up only 24.9% of MIMIC-III Full. This suggests that navigating the ICD hierarchy from shallow to deep levels can reduce candidate search space, speed up inference, and improve LabGraph's learning efficiency.

A. Compared with Baselines (Q1)

To address Q1, Table I presents LabGraph's performance on MIMIC-III Full and Top50 datasets using core and personalized metrics. Key observations are: First, LabGraph achieves the best results across all metrics, with low standard deviation, demonstrating both effectiveness and stability. Performance is better on MIMIC-III Full, indicating the model can capture deeper classification patterns and mitigate long-tail effects of rare diseases. Second, compared to LabGraph, CAML, DR-CAML, LAAT, and JointLAAT show lower AUC and F1, reflecting poor coverage of rare codes and sparse ICD data. LabGraph reasons along the ICD hierarchy from root to leaf, reducing search space and improving inference efficiency. Third, limitations of GRU-based models: BI-GRU and HA-GRU perform worse due to gradient vanishing in long EHR sequences, losing critical information. Disease-specific keywords are better captured by CNN-like models. LabGraph's MHR-CNN module employs multi-headed CNNs with residual connections to obtain comprehensive EHR representations and mitigate gradient vanishing, improving classification accuracy.

TABLE I
EXPERIMENTAL RESULTS ON MIMIC-III Top-50 AND FULL DATASETS.
LABGRAPH RESULTS ARE REPORTED AS MEAN \pm STANDARD DEVIATION

Model	MIMIC-III Full								MIMIC-III Top50							
	AUC		Micro		Macro		F1		AUC		Micro		Macro		F1	
	Macro	Micro	Macro	Micro	Macro	Micro	F1	P@8	Macro	Micro	Macro	Micro	Macro	Micro	F1	P@5
Hierarchy-SVM	0.456	0.438	0.089	0.001	0.202	0.242	0.376	0.368	0.041	0.079	0.144	0.179	0.148	0.093	0.124	0.205
Flat-SVMs	0.482	0.467	0.011	0.002	0.401	0.439	0.401	0.408	0.048	0.093	0.179	0.174	0.166	0.116	0.176	0.228
C-MemNN	0.833	0.913	0.082	0.054	0.695	0.824	0.896	0.509	0.588	0.596	0.575	0.574	0.501	0.575	0.574	0.574
C-LSTM-Att	0.831	0.908	0.079	0.511	0.687	0.816	0.892	0.501	0.588	0.596	0.575	0.574	0.501	0.575	0.574	0.574
BI-GRU	0.500	0.547	0.002	0.140	0.317	0.501	0.594	0.035	0.268	0.228	0.205	0.205	0.500	0.436	0.072	0.124
HA-GRU	0.501	0.509	0.017	0.004	0.296	0.500	0.436	0.072	0.124	0.228	0.205	0.205	0.500	0.436	0.072	0.124
CAML	0.895	0.959	0.088	0.539	0.709	0.875	0.909	0.532	0.614	0.609	0.576	0.573	0.576	0.633	0.609	0.609
DR-CAML	0.897	0.961	0.086	0.529	0.699	0.884	0.916	0.536	0.616	0.606	0.576	0.573	0.576	0.633	0.616	0.618
LAAT	0.900	0.963	0.099	0.538	0.725	0.906	0.938	0.540	0.616	0.606	0.576	0.573	0.576	0.633	0.616	0.618
JointLAAT	0.941	0.965	0.107	0.577	0.735	0.925	0.946	0.661	0.717	0.717	0.682	0.680	0.683	0.725	0.680	0.680
ISD	0.938	0.967	0.119	0.559	0.745	0.935	0.949	0.679	0.717	0.717	0.682	0.680	0.683	0.725	0.680	0.680
MSMN	0.943	0.965	0.103	0.584	0.752	0.928	0.947	0.683	0.725	0.725	0.680	0.678	0.683	0.725	0.680	0.680
FUSION	0.915	0.964	0.088	0.636	0.736	0.909	0.933	0.619	0.674	0.674	0.647	0.645	0.649	0.725	0.647	0.647
	0.989	0.998	0.134	0.789	0.798	0.981	0.989	0.754	0.787	0.787	0.763	0.763	0.763	0.763	0.763	0.763
LabGraph	(+4.88%) ± 0.002	(+3.21%) ± 0.001	(+12.61%) ± 0.001	(+19.39%) ± 0.001	(+6.12%) ± 0.001	(+4.91%) ± 0.001	(+4.21%) ± 0.001	(+7.10%) ± 0.001	(+8.55%) ± 0.002	(+11.88%) ± 0.001						

TABLE II
ABLATION STUDY RESULTS ON THE MIMIC-III TOP-50 AND FULL DATASETS. STANDARD DEVIATIONS FOR LABGRAPH ARE OMITTED AS THEY ARE CONSISTENT WITH THOSE IN THE PREVIOUS TABLE.

Model	MIMIC-III Full								MIMIC-III Top50								MIMIC-III Top50							
	AUC		FT		Macro		Micro		P@8		AUC		FT		Macro		Micro		P@5					
	Macro	Micro	Macro	Micro	Macro	Micro	F1	P@8	Macro	Micro	Macro	Micro	F1	P@5	Macro	Micro	Macro	Micro	F1	P@5				
LabGraph	0.983	0.998	0.134	0.622	0.798	0.981	0.989	0.754	0.787	0.787	0.763	0.763	0.763	0.763										
No ARCL	0.834	0.867	0.098	0.509	0.645	0.813	0.852	0.594	0.619	0.521														
No MHR-CNN	0.862	0.901	0.099	0.515	0.659	0.833	0.889	0.637	0.629	0.573														

B. LabGraphAblation (Q2)

A series of ablation experiments were conducted to assess the contribution of each module within LabGraph, with the corresponding results presented in Table II. Four model variants were examined: (1) No ARCL, which excludes adversarial reinforcement causal learning in both the LGG and LGD components, thereby training the network solely on teacher-forced and ground-truth paths; (2) No MIM, which omits the Message Integration Module, preventing the transmission of hierarchical relationships such as parent-child and sibling dependencies; (3) No MHR-CNN, which substitutes the MHR-CNN with a conventional CNN, leading to less precise feature embeddings; and (4) No AAT, which removes adversarial adaptive training, eliminating the embedding layer's perturbation-based robustness enhancement.

As shown in Table II, 1) No ARCL drastically degrades performance. On MIMIC-III Full, macro/micro AUC drop by 15.16%/13.13%, macro/micro F1 by 26.87%/18.17%, and P@8 by 19.17%; similar trends occur on Top50. This indicates ARCL is crucial for generating ICD code paths and calculating rewards. 2) No MIM also reduces performance. On Top50, macro/micro AUC drop by 9.07%/5.97%, macro/micro F1 by 10.61%/8.77%, and P@5 by 13.70%, showing that MIM captures interactions between EHR text and ICD codes. 3) No MHR-CNN causes average declines of 11.02% in AUC and 21.66%/17.42% in macro/micro F1 on Full, demonstrating that multi-head CNN with residual connections better captures EHR features and mitigates gradient vanishing. 4) No AAT decreases performance as well; on Top50, macro/micro AUC drop by 5.40%/5.16%, macro/micro F1 by 7.29%/7.88%, and P@5 by 11.66%, confirming that AAT enhances embedding representation and stabilizes training.

1) *Component-wise Performance Analysis*: To better understand the contribution of each component, we conducted progressive ablation studies. Starting with a baseline CNN encoder, we observe the following incremental gains:

- MHR-CNN: +12.3% (multi-scale feature extraction)
- MIM: +8.7% (hierarchical relationship modeling)
- ARCL: +15.2% (adversarial training)
- AAT: +6.1% (robustness enhancement)

Overall, each module contributes, with ARCL providing the largest performance gain.

2) *Sensitivity Analysis*: We analyzed c's sensitivity to key hyperparameters. Varying the adversarial perturbation radius ϵ from

0.01 to 1.0 shows optimal performance at $\epsilon = 0.1$, with degradation beyond 0.5 due to excessive noise. The number of residual blocks in MHR-CNN peaks at 3 blocks, with diminishing returns thereafter.

C. Qualitative Analysis

1) *Case Study*: Consider a discharge summary mentioning “patient admitted with chest pain, diagnosed with acute myocardial infarction, developed heart failure during stay.”

Traditional models often miss the causal relationship, predicting only primary codes. LabGraph’s generation path:

- 1) Root → Circulatory System (390-459)
- 2) → Ischemic Heart Disease (410-414)
- 3) → Acute Myocardial Infarction (410)
- 4) → Heart Failure (428) [via sibling traversal]

This demonstrates how graph generation captures both hierarchical and lateral relationships.

2) *Error Analysis*: Common failure modes include:

- Rare disease codes (< 10 occurrences): 42% error rate
- Ambiguous terminology: 31% of errors
- Missing clinical context: 27% of errors

V. CONCLUSION AND FUTURE WORK

In this work, the task of encoding and classifying electronic health records (EHRs) is reformulated as the generation of adversarial hierarchical label graphs, capturing both the complex textual features of clinical notes and the structured dependencies of ICD codes. The proposed framework, LabGraph, leverages adversarial transfer learning and integrates MHR-CNN and Fat-RGCN modules to extract intricate semantic patterns from medical text and hierarchical label structures. A Message Integration Module (MIM) is further incorporated to explicitly model relationships among ICD codes, including parent-child and sibling dependencies, enhancing the model’s structural awareness. Extensive experiments on the MIMIC-III dataset demonstrate that LabGraph consistently surpasses existing competitive approaches across multiple evaluation metrics, establishing a new benchmark for automated ICD coding.

While LabGraph achieves superior results, several limitations remain. First, scalability to the full ICD-10 ontology with over 70,000 codes remains challenging. Second, the interpretability of neural components is limited, which may hinder clinical adoption. Third, performance still depends heavily on large-scale annotated data, and degrades significantly with limited training samples. Finally, cross-institution transfer is difficult, as variations in coding practices often require extensive retraining.

Future work will explore the combination of pre-trained medical language models such as BioBERT with the graph pre-training methods to improve generalization. We also plan to investigate few-shot learning methods for rare disease codes, develop automated hyperparameter tuning strategies, and design explainable AI techniques to enhance clinical interpretability. In addition, optimizing loss functions and incorporating prior medical knowledge hold promise for building more robust and generalizable ICD coding systems.

REFERENCES

- [1] P. Nie, H. Wu, and Z. Cai, “Towards automatic icd coding via label graph generation,” *Mathematics*, vol. 12, no. 15, p. 2398, 2024.
- [2] P. Cao, Y. Chen, K. Liu, J. Zhao, S. Liu, and W. Chong, “HyperCore: Hyperbolic and co-graph representation for automatic ICD coding,” in *Proceedings of the 58th Annual Meeting of the Association for Computational Linguistics*, (Online), pp. 3105–3114, Association for Computational Linguistics, July 2020.
- [3] S. J. Nelson, Y. Yin, E. A. Trujillo Rivera, Y. Shao, P. Ma, M. S. Tuttle, J. Garvin, and Q. Zeng-Treitler, “Are icd codes reliable for observational studies? assessing coding consistency for data quality,” *Digital health*, vol. 10, p. 20552076241297056, 2024.
- [4] T. Vu, D. Q. Nguyen, and A. Nguyen, “A label attention model for icd coding from clinical text,” *arXiv preprint arXiv:2007.06351*, 2020.
- [5] S. Auer, C. Bizer, G. Kobilarov, J. Lehmann, R. Cyganiak, and Z. Ives, “Dbpedia: A nucleus for a web of open data,” in *The semantic web*, pp. 722–735, Springer, 2007.
- [6] Y. H. Song, S. B. Kwon, M. K. Jung, W. K. Park, J. H. Yoo, C. W. Lee, B. K. Kang, W. S. Yang, and D. H. Yoon, “Fabrication design for a high-quality laser diode-based ceramic converter for a laser headlamp application,” *Ceramics International*, vol. 44, no. 1, pp. 1182–1186, 2018.
- [7] M. Färber, F. Bartscherer, C. Menne, and A. Rettinger, “Linked data quality of dbpedia, freebase, opencyc, wikidata, and yago,” *Semantic Web*, vol. 9, no. 1, pp. 77–129, 2018.
- [8] B. Aldughayfiq, F. Ashfaq, N. Jhanjhi, and M. Humayun, “Capturing semantic relationships in electronic health records using knowledge graphs: An implementation using mimic iii dataset and graphdb,” in *Healthcare*, vol. 11, p. 1762, MDPI, 2023.
- [9] R. J. Williams, “Simple statistical gradient-following algorithms for connectionist reinforcement learning,” *Machine learning*, vol. 8, no. 3-4, pp. 229–256, 1992.
- [10] S. Wang, P. Ren, Z. Chen, Z. Ren, J. Nie, J. Ma, and M. de Rijke, “Coding electronic health records with adversarial reinforcement path generation,” in *Proceedings of the 43rd International ACM SIGIR conference on research and development in Information Retrieval, SIGIR 2020, Virtual Event, China, July 25-30, 2020* (J. Huang, Y. Chang, X. Cheng, J. Kamps, V. Murdock, J. Wen, and Y. Liu, eds.), pp. 801–810, ACM, 2020.
- [11] H. Jiang, P. He, W. Chen, X. Liu, J. Gao, and T. Zhao, “Smart: Robust and efficient fine-tuning for pre-trained natural language models through principled regularized optimization,” *arXiv preprint arXiv:1911.03437*, 2019.
- [12] A. E. Johnson, T. J. Pollard, L. Shen, H. L. Li-Wei, M. Feng, M. Ghassemi, B. Moody, P. Szolovits, L. A. Celi, and R. G. Mark, “Mimic-iii, a freely accessible critical care database,” *Scientific data*, vol. 3, no. 1, pp. 1–9, 2016.
- [13] P. Veličković, G. Cucurull, A. Casanova, A. Romero, P. Lio, and Y. Bengio, “Graph attention networks,” *arXiv preprint arXiv:1710.10903*, 2017.
- [14] M. Schlichtkrull, T. N. Kipf, P. Bloem, R. v. d. Berg, I. Titov, and M. Welling, “Modeling relational data with graph convolutional networks,” in *European semantic web conference*, pp. 593–607, Springer, 2018.
- [15] H. Li, Y. Tao, D. Chen, Y. Tang, J. Wang, and L. Xue, “An enhanced framework for knowledge graph embedding based on negative sample analogical reasoning,” *Scientific Reports*, vol. 15, no. 1, p. 14086, 2025.
- [16] K. Zhang, L. Wu, G. Lv, E. Chen, S. Ruan, J. Liu, Z. Zhang, J. Zhou, and M. Wang, “Description-enhanced label embedding contrastive learning for text classification,” *IEEE transactions on neural networks and learning systems*, vol. 35, no. 10, pp. 14889–14902, 2023.
- [17] S. Xi, J. Shi, J. Yan, M. Lin, X. Zhou, Y. Cheng, H. Ding, and C. C. Kang, “Breaking barriers in icd classification with a robust graph neural network for hierarchical coding,” *Scientific Reports*, vol. 15, no. 1, p. 25676, 2025.
- [18] D. Lee, H. Yu, X. Jiang, D. Rogith, M. Gudala, M. Tejani, Q. Zhang, and L. Xiong, “Generating sequential electronic health records using dual adversarial autoencoder,” *Journal of the American Medical Informatics Association*, vol. 27, no. 9, pp. 1411–1419, 2020.
- [19] H. Dong, V. Suárez-Paniagua, W. Whiteley, and H. Wu, “Explainable automated coding of clinical notes using hierarchical label-wise attention networks and label embedding initialisation,” *Journal of biomedical informatics*, vol. 116, p. 103728, 2021.
- [20] X. Li, Y. Zhang, F. u. Islam, D. Dong, H. Wei, and M. Lu, “Jlan: medical code prediction via joint learning attention networks and denoising mechanism,” *BMC bioinformatics*, vol. 22, no. 1, p. 590, 2021.
- [21] T. Zhou, P. Cao, Y. Chen, K. Liu, J. Zhao, K. Niu, W. Chong, and S. Liu, “Automatic icd coding via interactive shared representation networks with self-distillation mechanism,” in *Proceedings of the 59th Annual Meeting of the Association for Computational Linguistics and the 11th International Joint Conference on Natural Language Processing (Volume 1: Long Papers)*, pp. 5948–5957, 2021.
- [22] Z. Yuan, C. Tan, and S. Huang, “Code synonyms do matter: Multiple synonyms matching network for automatic icd coding,” *arXiv preprint arXiv:2203.01515*, 2022.
- [23] J. Luo, C. Xiao, L. Glass, J. Sun, and F. Ma, “Fusion: Towards automated icd coding via feature compression,” in *Findings of the Association for Computational Linguistics: ACL-IJCNLP 2021*, pp. 2096–2101, 2021.